^{1}H NMR Study of Rabbit Skeletal Muscle Troponin C: Mg^{2+}-Induced Conformational Change†

Sakae Tsuda,*,‡ Kenji Ogura, Yasushi Hasegawa,§ Koichi Yagi,§,∥ and Kunio Hikichi
Department of Polymer Science and Department of Chemistry, Faculty of Science, Hokkaido University, Sapporo 060, Japan
Received August 16, 1989; Revised Manuscript Received December 28, 1989

ABSTRACT: Binding of Mg^{2+} to rabbit skeletal muscle troponin C (TnC) is studied by means of two-dimensional (2D) ^{1}H NMR spectroscopy. Using the sequence-specific resonance assignment method we assign several resonances of TnC in the Mg^{2+}-saturated state. Assigned resonances are used as probes of the following titration experiments: (1) Mg^{2+} titration of apo-TnC, (2) Mg^{2+} titration of Ca_2TnC, and (3) Mg^{2+} titration of Ca_4TnC. In experiment 1, the slow-exchange behavior is observed for resonances of Phe99, Asp107, Gly108, Tyr109, Ile110, Asp111, His125, Gly144, Arg145, Ile146, Asp147, and Phe148 located at the high-affinity Ca^{2+}-binding sites in the C-terminal-half domain. In experiments 1 and 2, the fast-exchange behavior is observed for resonances of Gly32, Asp33, Ser35, Gly68, Thr69, and Asp71 located at the low-affinity Ca^{2+}-binding sites in the N-terminal-half domain. These results suggest that Mg^{2+} ions bind to the N domain as well as the C domain. In experiment 3, no spectral change is observed for all above-mentioned residues in the C domain and also for Gly32 and Gly68 in the N domain. It can be concluded that all Ca^{2+}-binding sites in both the N and C domains can bind Mg^{2+} ions. No significant change is observed for resonances of Phe23, Ile34, Val68, and Phe72 in experiments 1 and 2. These results suggest that Mg^{2+} binding to the N domain does not induce conformational change in the hydrophobic region of the N domain. 2D-NMR spectra and Mg^{2+}-titration data suggest that the antiparallel β-sheet conformation is formed in both the N and C domains when Mg^{2+} ions bind to the two domains.

Rabbit skeletal muscle troponin C (TnC)[1] (MW = 17965; 159 residues) binds 4 mol of Ca^{2+} per mol of protein (Collins et al., 1975). The structure of TnC in the crystal has been solved and reveals a dumbbell-shaped molecule with two globular N- and C-terminal-half domains jointed by an α-helical bridge (Herzberg & James, 1988). In each globular domain, there are two pairs of "helix–loop–helix" Ca^{2+}-binding sites; each participates in a short antiparallel β-sheet structure (Babu et al., 1987). The C domain binds 2 mol of Ca^{2+} with high affinity ($K_{Ca^{2+}} = 2.1 \times 10^7$ M^{-1}) and the N domain binds 2 mol of Ca^{2+} with low affinity ($K_{Ca^{2+}} = 3.2 \times 10^5$ M^{-1}) [see the review by Vogel et al. (1983)]. Potter and Gergely (1975) showed that the two high-affinity Ca^{2+} sites also bind 2 mol of Mg^{2+}. Thus, the high-affinity Ca^{2+} sites have been called "Ca^{2+}–Mg^{2+} sites". On the other hand, the low-affinity Ca^{2+} sites were reported not to bind Mg^{2+} and are called "Ca^{2+}-specific sites" (Potter & Gergely, 1975; Grabarek et al., 1986). However, Kohama (1980) and Ogawa (1985) showed that Mg^{2+} ions bind to the low-affinity Ca^{2+} sites as well as the high-affinity Ca^{2+} sites; the low-affinity Ca^{2+} sites are not specific to Ca^{2+} ions.

There have been a number of ^{1}H NMR studies on TnC. It has been shown that the conformation of TnC changes when 4 mol of Ca^{2+} binds to the protein [see the reviews of Ribeiro et al. (1984) and Tsuda et al. (1988)]. The Mg^{2+}-induced conformational change of TnC was studied by Levine et al. (1978). They reported that the binding of Mg^{2+} to TnC does not induce conformational change in the N domain and concluded that Mg^{2+} does not bind to the low-affinity Ca^{2+} sites. Levine et al. (1978) and Drabikowski et al. (1985) noted some differences in conformation of the C domain between the Ca^{2+}-bound form and the Mg^{2+}-bound form, though they admitted overall similarity. Andersson et al. (1981) reported on the basis of an ^{25}Mg NMR study that there exist Mg^{2+}-binding sites in addition to the Ca^{2+}–Mg^{2+} sites. All these published results indicate that Mg^{2+} binding to TnC is not understood well.

Previous conclusions of ^{1}H NMR studies on TnC in the Mg^{2+}-saturated state have been based on a small number of assigned resonances (Levine et al., 1978; Drabikowski et al., 1985; Drakenberg et al., 1987). In the present work, we attempted to assign resonances of TnC in the Mg^{2+}-saturated state as possible, by observing two-dimensional (2D) NMR spectra. We confirmed the previous assignments and made a number of additional assignments on the basis of the sequence-specific resonance assignment method (Billeter et al., 1982; Wüthrich et al., 1982, 1984; Wüthrich, 1983). Assigned resonances were used to monitor Mg^{2+}-binding to TnC. The disposition of β-sheet structure and hydrogen bond in Mg^{2+}-saturated TnC was discussed in terms of the recent X-ray crystal structure of turkey skeletal muscle TnC (Herzberg & James, 1988).

Materials and Methods

Rabbit skeletal muscle TnC was prepared by published procedure (Szynkiewicz et al., 1984).

^{1}H NMR experiments were carried out on JEOL JNM GX-400 and GX-500 spectrometers operating at frequencies of 400 and 500 MHz, respectively, at a temperature of 40 °C.

† This work was supported by Grants-in-Aid for Scientific Research from the Ministry of Education, Science, and Culture of Japan (61230002, 62220001, and 63111005).
‡ Department of Polymer Science.
§ Department of Chemistry.
∥ Present address: Department of Food Science, Rakuno Gakuen University, Ebetsu 069, Japan

[1] Abbreviations: NMR, nuclear magnetic resonance; 2D, two dimensional; 2QF-COSY, double quantum filtered correlated spectroscopy; NOESY, nuclear Overhauser enhancement effect spectroscopy; DANTE, delayed alternating with nutations for tailored excitation; SR-1331, self-refocused-1331; TnC, calcium binding subunit of troponin; Ca_2TnC, TnC with 2 mol of calcium at the high-affinity sites; Ca_4TnC, TnC with 4 mol of calcium at the high- and low-affinity sites; CaM, calmodulin; DTT, dithiothreitol; TSP, (trimethylsilyl)propionic-d_4 acid sodium salt.

0006-2960/90/0429-4951$02.50/0

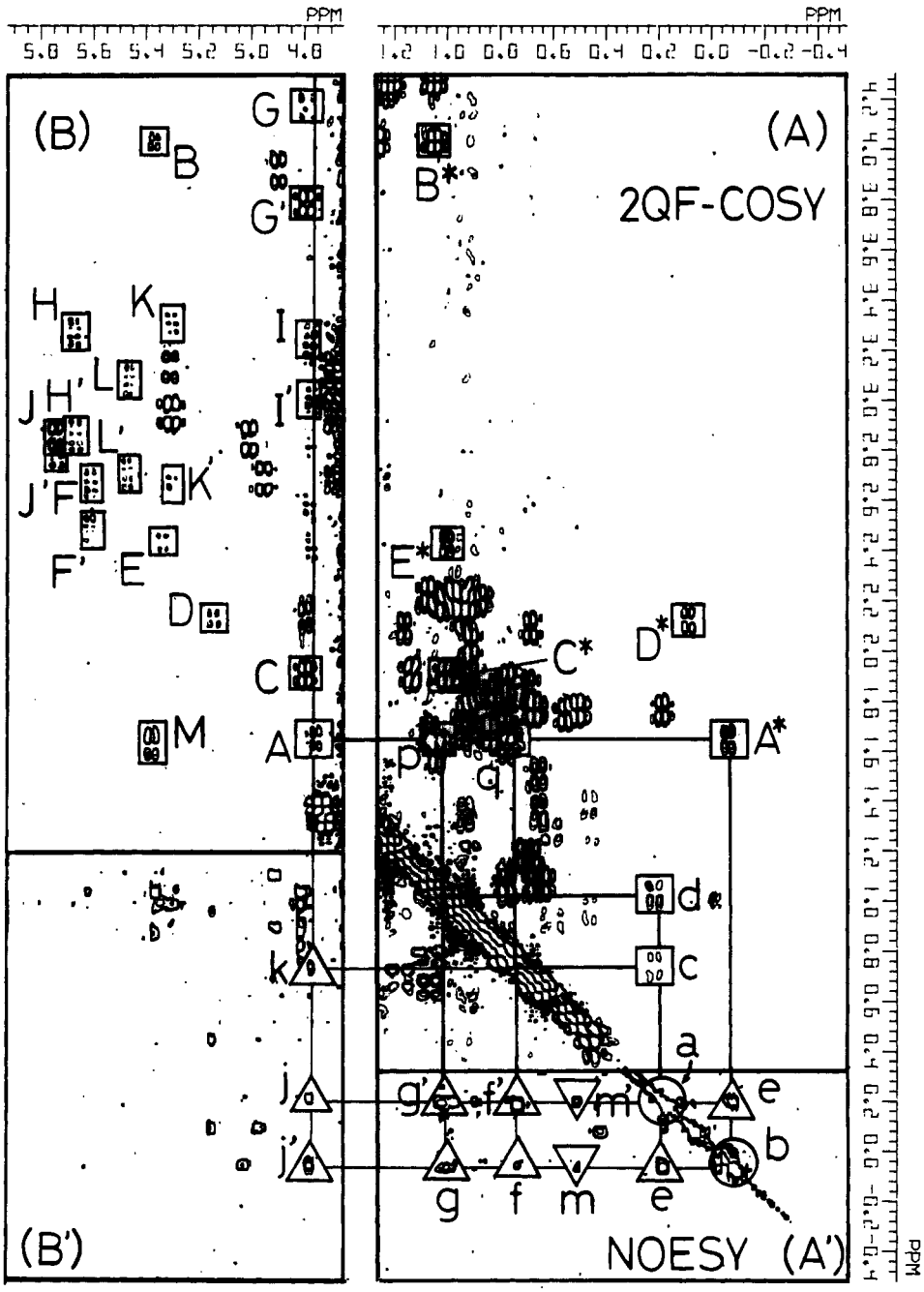

FIGURE 1: Expansions of the pure-phase 2QF-COSY spectrum (A and B) and the pure-phase NOESY spectrum (A′ and B′) of rabbit skeletal muscle TnC in the Mg^{2+}-saturated state (D_2O, [TnC] ≅ 5 mM, [Mg^{2+}] = 180 mM, [KCl] = 200 mM, [DTT] = 50 mM, pH 6.9, 40 °C, 400 MHz; mixing time for NOESY is 180 ms). Assignments of labeled cross-peaks are indicated in the text and Table I.

TnC was dissolved in D_2O at a concentration of 1.6 mM for Mg^{2+}- and pH-titration experiments. Mg^{2+} ions were added up to a ratio [Mg^{2+}]/[TnC] of about 32. pH was adjusted at a temperature of 24 °C and reported without deuterium correction. For 2D NMR experiments, 12 mM TnC was dissolved in H_2O/D_2O (90/10) but resulted in precipitation. The final concentration was not known exactly but estimated to be about 5 mM from NMR spectra. All solutions contain 200 mM KCl. Dithiothreitol (DTT) (15–50 mM) was added to prevent dimerization of TnC.

2QF-COSY, HOHAHA, and NOESY spectra were observed in the pure-phase mode (Müller et al., 1986; Bax et al., 1981; Bax & Davis, 1985). For NOESY experiments the mixing time was changed from 100 to 200 ms. The mixing time ranging from 20 to 150 ms was used for HOHAHA experiments. Water-peak suppression was achieved by gated irradiation in 2QF-COSY experiment and DANTE irradiation in NOESY experiments (Zuiderweg et al., 1986). Some of NOESY spectra were obtained by applying the SR-1331 pulse sequence for water-peak suppression (Takegoshi et al., 1989). No sample spinning was applied (Mehlkopf et al., 1984). A time domain data matrix of 256 × 1024 points was in most cases expanded to 512 × 2048 points by "zero filling". All 2D data were apodized by using a gauss-exponential window function in the t_2 dimension and a shifted sine-bell window function in the t_1 dimension. T_1 noise in pure-phase NOESY spectra was suppressed by the t_1 ridge subtraction method (Klevit, 1985).

Results and Discussion

Assignments of TnC in the Mg^{2+}-Saturated State and the Apo State. The right-hand part of Figure 1 represents high-field methyl–methylene regions of a pure-phase 2QF-COSY spectrum (upper frame, A) and a pure-phase NOESY

spectrum (lower frame, A′) of TnC in D_2O at a $[Mg^{2+}]/[TnC]$ ratio of 36. The left-hand part represents a methine–methylene region of the pure-phase 2QF-COSY spectrum (upper frame, B) and a methine–methyl region of the pure-phase NOESY spectrum (lower frame, B′). Figure 1A shows that methyl proton resonance a at 0.24 ppm is connected to cross-peaks c and d of two unequivalent methylene proton resonances. These connectivities are attributed to a scalar-coupling network of $C^{\delta}H_3$ protons and two $C^{\gamma}H_2$ protons of an Ile (IleA). Cross-peak A* shows a J connectivity between $C^{\gamma}H_3$ resonance b at −0.10 ppm and a methine proton resonance at 1.67 ppm (diagonal data not shown). The latter is connected to the two $C^{\gamma}H_2$ protons of IleA as indicated by cross-peaks p and q. Thus, resonance b is assigned to the $C^{\gamma}H_3$ protons of IleA. In the NOESY spectrum of Figure 1A′ we see an intraresidue NOE connectivity between $C^{\delta}H_3$ resonance a and $C^{\gamma}H_3$ resonance b of IleA as evidenced by cross-peak e. Cross-peaks f and g are also intraresidue NOE peaks between $C^{\gamma}H_3$ protons b and the two $C^{\gamma}H_2$ protons of IleA. Cross-peak f′ shows an NOE connectivity between the $C^{\delta}H_3$ protons and one of the unequivalent $C^{\gamma}H_2$ protons and g′ shows the connectivity between the $C^{\delta}H_3$ protons and the other proton of $C^{\gamma}H_2$. Cross-peaks m and m′ are attributed to interresidue NOE connectivities between the $C^{\gamma}H_3$ protons of IleA and a methyl group of Val62 (see below), respectively.

As shown in the 2QF-COSY spectrum of Figure 1B, the $C^{\alpha}H$ proton resonance of IleA can be readily identified by cross-peak A, which represents a connectivity between the $C^{\beta}H$ proton at 1.67 ppm and the $C^{\alpha}H$ proton at 4.76 ppm. In the NOESY spectrum of Figure 1B′, cross-peak j shows an intraresidue NOE connectivity between the $C^{\alpha}H$ proton and the $C^{\delta}H_3$ protons of IleA, and cross-peak K is due to the intraresidue NOE between the $C^{\alpha}H$ and one of the $C^{\gamma}H_2$ protons of IleA. Cross-peak j′ represents the intraresidue NOE between the $C^{\alpha}H$ proton and a $C^{\gamma}H_3$ proton.

The combined use of HOHAHA and 2QF-COSY indicates that cross-peaks labeled B, C, D, and E are due to J connectivities between $C^{\alpha}H$ and $C^{\beta}H$ of four xxx residues (xxx1, xxx2, xxx3, and xxx4), which are of Thr or Ile. Cross-peaks labeled B*, C*, D*, and E* are due to J connectivities between $C^{\beta}H$ and $C^{\gamma}H_3$ of xxx residues. Cross-peaks labeled F, F′, G, G′, ..., L, and L′ show J connectivities between $C^{\alpha}H$ and $C^{\beta}H_2$ of seven AMX-type residues which include Asp, Asn, Cys, His, Ser, Tyr, and Phe (Wüthrich, 1976). The combined use of 2QF-COSY, HOHAHA, and NOESY reveals spin systems of four Phe's (PheA, PheB, PheC, and PheD) out of 10 and both Tyr's (TyrA and TyrB). Cross-peaks j and j′ are assigned to TyrA. The cross-peak labeled M in Figure 1B belongs to the spin system of the yyy residue, which is of Arg, Lys, Met, Glu, or Gln. Details of assignments of the above-mentioned residues are shown in the supplementary material.

Figure 2 shows expansions of 2QF-COSY (lower) and NOESY (upper) spectra of TnC in H_2O at a $[Mg^{2+}]/[TnC]$ ratio of 36. In the 2QF-COSY spectrum, ($C^{\alpha}H$, NH) cross-peaks of TyrA, IleA, yyy, and three AMX-type residues, AMX1, AMX2, and AMX3, are labeled. Vertical pairs of ($C^{\alpha}H$, NH) cross-peaks in the 2QF-COSY spectrum are typical for Gly's. We identify four Gly's: GlyA, GlyB, GlyC, and GlyD. Vertical broken lines drawn from the above-mentioned cross-peaks point to positions of amide proton resonances in the NOESY spectrum. To avoid congestion, lines are not drawn from IleA and AMX3. Because solid squares in the NOESY spectrum show NOE d_{NN} connectivities of two sequentially adjacent residues, the following peptide segments are identified; GlyA-GlyB-AMX1, GlyD-yyy, and

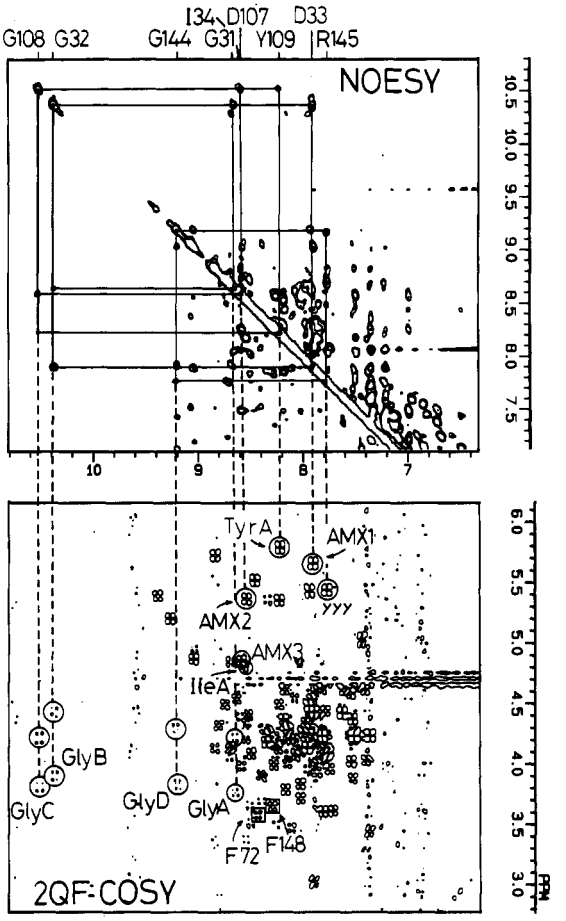

FIGURE 2: Expansions of the pure-phase 2QF-COSY spectrum (lower part) and the pure-phase NOESY spectrum of rabbit skeletal muscle TnC in the Mg^{2+}-saturated state (H_2O:D_2O = 9:1, [TnCl] ≅ 5 mM, $[Mg^{2+}]$ = 180 mM, [KCl] = 200 mM, [DTT] = 50 mM, pH 6.9, 40 °C, 500 MHz; mixing time for NOESY is 100 ms). Water suppression was achieved by the SR-1331 pulse. Vertical broken lines connect ($C^{\alpha}H$, NH) 2QF-COSY cross-peaks with their amide resonances. Two adjacent residues are assigned through NOE d_{NN} connectivities illustrated by solid squares.

AMX2-GlyC-TyrA. The latter segment is assigned to Asp^{107}-Gly^{108}-Tyr^{109} by reference to the amino acid sequence.

Figure 3A shows an amide-$C^{\alpha}H$ region of NOESY spectrum of TnC in H_2O at a $[Mg^{2+}]/[apo\text{-}TnC]$ ratio of 36. The one-dimensional spectrum is shown at the top and also at the right. Triangles with numbers show the positions of ($C^{\alpha}H$, NH) cross-peaks of the 2QF-COSY spectrum. Triangles 33, 34, and 35 correspond respectively to AMX1, IleA, and AMX3 shown in Figure 2. Since NOESY cross-peaks marked by I and II represent $d_{\alpha N}$ connectivities between 33 and 34 and between 34 and 35, respectively, AMX1, IleA, and AMX3 are found to be sequentially connected (indicated by arrows). Combination of this segment with the segment GlyA-GlyB-AMX1 identified above gives a pentapeptide segment of GlyA-GlyB-AMX1-IleA-AMX3. Inspection of the amino acid sequence indicates that this segment is Gly^{31}-Gly^{32}-Asp^{33}-Ile^{34}-Ser^{35}.

Figure 3B is the same pure-phase NOESY spectrum as Figure 3A and illustrates the $d_{\alpha N}$ connectivities for other residues. Triangle 109 is a COSY-type ($C^{\alpha}H$, NH) cross-peak of Tyr109 (TyrA). Triangles 110 and 111 correspond to xxx1 and AMX4 mentioned before, respectively. By NOE $d_{\alpha N}$ connectivities, a segment Tyr^{109}-xxx1-AMX4 is found. Thus, we have a segment Asp^{107}-Gly^{108}-Tyr^{109}-Ile^{110}(xxx1)-Asp^{111}-(AMX4). Position of the 2QF-COSY ($C^{\alpha}H$, NH) cross-peak of yyy is out of the frame of Figure 3B and shown in Figure

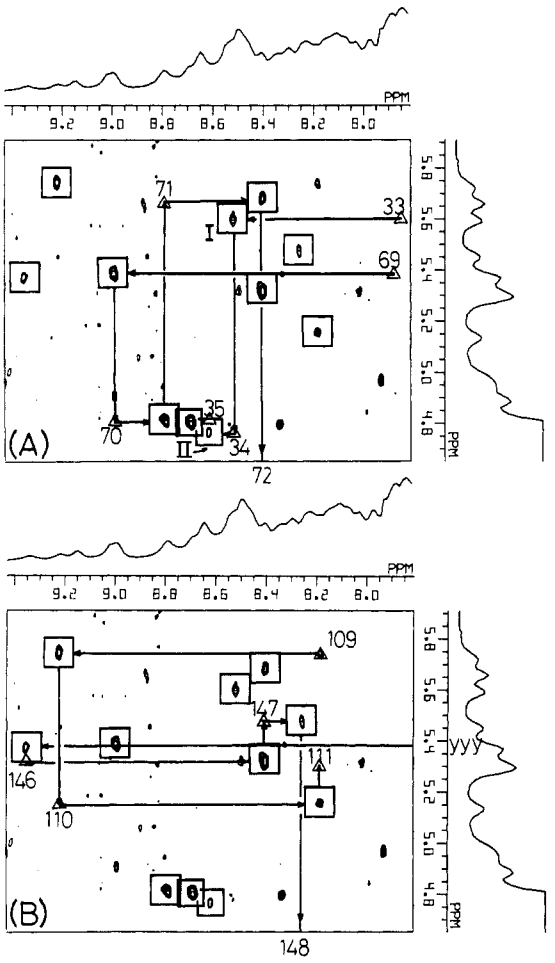

FIGURE 3: Upper and lower spectra are the same expansions of pure-phase NOESY spectra with DANTE irradiation of TnC in the Mg^{2+}-saturated state. The mixing time used was 100 ms. Other experimental conditions are same as described in Figure 2. One-dimensional spectra of the same region are shown at the top and at the right. Positions of some ($C^{\alpha}H$, NH) 2QF-COSY cross-peaks are indicated by triangles. Horizontal lines represent the NOESY $d_{\alpha}N$ connectivities between residue i and residue $i + 1$. The vertical lines indicate the position of ($C^{\alpha}H$, NH) 2QF-COSY cross-peaks.

2. This is sequentially connected to 146(xxx2), 147(AMX5), and 148 (out of frame; PheD) as indicated by arrows. Thus, the segment GlyD-yyy shown in Figure 2 is extended to GlyD-yyy-xxx2-AMX5-PheD, which is assigned to Gly^{114}-Arg^{145}-Ile^{146}-Asp^{147}-Phe^{148}. In the same way, a segment Thr^{69}-Ile^{70}-Asp^{71}-Phe^{72} is identified in Figure 3A. Positions of 2QF-COSY cross-peaks of Phe148 and Phe72 are also shown in Figure 2. Some assigned amide protons are indicated in the upper part of NOESY by the IUB-IUPAC one-letter symbol with the number of the location in the sequence.

Since Tyr109 resonance is determined, Tyr10, which is another tyrosine in TnC, is automatically assigned. Table I lists chemical shifts of some assigned resonances in the present work.

In the present study, the previous assignments of Phe72 and Phe23 of apo-TnC were found to be erroneous and should be interchanged (this revision does not change any conclusion of the previous paper) (Tsuda et al., 1988). It was also found in the apo state that Thr69 assigned in the previous paper is connected to glycine, i.e., Gly68.

Mg^{2+} Titration of Apo-TnC. We carried out the Mg^{2+}-titration experiment for apo-TnC. Figure 4 shows an aromatic region of the ^1H NMR spectra of TnC at various Mg^{2+} concentrations. Numbers at the left-hand side indicate the molar ratio of $[Mg^{2+}]/[apo\text{-}TnC]$.

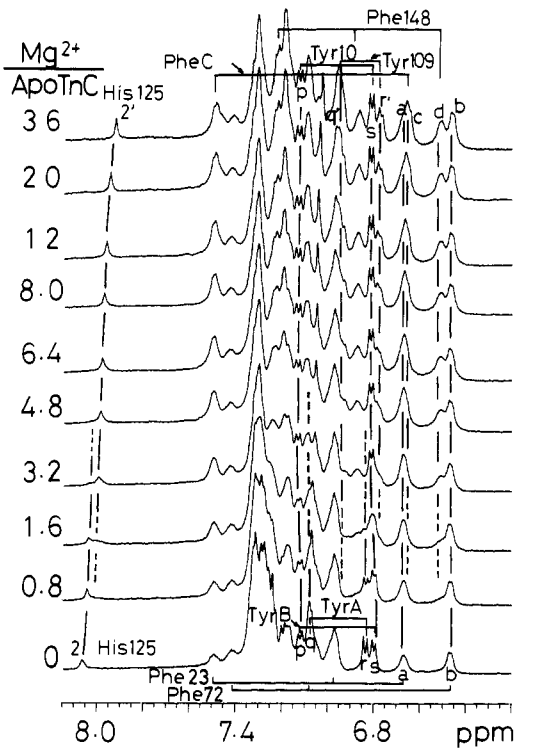

FIGURE 4: Aromatic region of ^1H NMR spectra of rabbit skeletal muscle TnC at various concentrations of Mg^{2+} added to apo-TnC (D_2O, [TnC] = 1.6 mM, [DTT] = 18 mM, [KCl] = 200 mM, pH 7.5–7.8, 40 °C, 500 MHz).

C2 and C4 ring protons of His125 (TnC has only one histidine at the 125th position) were assigned by pH titration in both apo and Mg^{2+}-saturated states. With increasing ratio of $[Mg^{2+}]/[apo\text{-}TnC]$ from 0 to 4.8, the C2 proton resonance of His125 (peak 2) decreases in intensity and disappears. In parallel with this decrease, a new resonance (peak 2′) appears at 7.98 ppm and increases in intensity. A continuous change in chemical shift of peaks 2 and 2′ reflects a change in pH. The addition of Mg^{2+} causes a small change in pH from 7.5 to 7.8.

In the preceding section, the resonances c (6.67 ppm) and d (6.52 ppm) in the top spectrum of Figure 4 for Mg^{2+}-saturated TnC were assigned respectively to δ-ring protons of PheC and Phe148. In the course of the Mg^{2+} titration, these two resonances change in intensity. For apo-TnC these resonances are probably located in the crowded region of 7.0–7.3 ppm.

With increasing ratio of $[Mg^{2+}]/[apo\text{-}TnC]$ from 0 to 36, the doublet resonances p at 7.12 ppm and s at 6.80 ppm broaden and shift to 7.14 ppm and 6.85 ppm, respectively. These resonances p and s for apo-TnC were assigned respectively to $C^{\epsilon}H$ and $C^{\delta}H$ of TyrB in a previous paper (Tsuda et al., 1988). In the Mg^{2+}-saturated state, resonances p and s in the top spectrum were assigned to the ring protons of Tyr10 as described previously. Therefore, TyrB of apo-TnC shown at the bottom is Tyr10. Another TyrA of apo-TnC is automatically assigned to Tyr109.

With increasing $[Mg^{2+}]/[apo\text{-}TnC]$ ratio from 0 to 4.8, peak r (6.83 ppm) and peak q (7.07 ppm) of Tyr109(TyrA) decrease in intensity and disappear above $[Mg^{2+}]/[apo\text{-}TnC] \sim 3$. In parallel with the decrease, alternative ring proton resonances of Tyr109 appear at 6.78 and 7.12 ppm and increase in intensity.

As shown in Figure 4, the resonances of δ- and ϵ-ring protons of Tyr10 change chemical shifts in the range of $[Mg^{2+}]/[apo\text{-}TnC]$ ratio from 0 to 4.8. On the other hand, the reso-

Table I: Chemical Shifts (ppm) of Assigned Resonances of Rabbit Skeletal Muscle Troponin C in the Mg^{2+}-Bound State[a]

residue	no.	NH	α	β	others
Tyr	10		4.44	3.60, 3.06	6.85 (δ), 7.14 (ε)
Phe	23+	8.34	3.70	3.28, 2.82	6.70 (δ), 7.00 (ε), 7.50 (ζ)
Gly	31	8.60	4.20, 3.80		
Gly	32	10.32	4.40, 3.85		
Asp	33	7.84	5.61	2.64^{F}, $2.48^{F'}$	
Ile	34	8.53	4.76	1.67^{A}	(0.73, 1.05) $(\gamma)^{A*}$, −0.10 (γ), 0.24 (δ)
Ser	35	8.64	4.79	4.18^{G}, $3.81^{G'}$	
Val	62+		3.53	1.77	(0.56, 0.78) (γ)
GlyB	68+	10.22			
Thr	69	7.88	5.38	4.05^{B}	1.05 $(\gamma)^{B*}$
Ile	70	9.00	4.82	1.92^{C}	1.04 $(\gamma)^{C*}$
Asp	71	8.78	5.68	3.25^{H}, $2.87^{H'}$	
Phe	72	8.40	3.54	2.69, 2.48	6.49 (δ), 7.13 (ε), 7.43 (ζ)
PheC	99+		3.45	2.53, 2.18	6.67 (δ), 7.26 (ε), 7.30 (ζ)
Asp	107	8.54	4.80	3.25^{I}, $3.00^{I'}$	
Gly	108	10.48	4.15, 3.52		
Tyr	109	8.18	5.74	2.89^{J}, $2.75^{J'}$	6.78 and 6.88 (δ and ε or vice versa)
Ile	110	9.24	5.16	2.12^{D}	0.08 $(\gamma)^{D*}$
Asp	111	8.18	5.30	3.30^{K}, $2.68^{K'}$	
His	125		4.60	3.02	8.06 (C2), 7.16 (C4)
Gly	144	9.18	3.80, 4.20		
Arg	145	7.72	5.39	1.61^{M}	
Ile	146	9.34	5.33	2.45^{E}	1.01 $(\gamma)^{E*}$
Asp	147	8.40	5.47	3.08^{L}, $2.68^{L'}$	
Phe	148	8.26	3.60	3.24, 2.90	6.52 (δ), 6.90 (ε), 7.25 (ζ)

[a] Experimental conditions are as follows: [TnC] ~ 5 mM; [KCl] = 0.2 M; [DTT] = 50 mM; 40 °C. Data for amide protons are obtained in H_2O (H_2O:D2O = 9:1, pH 6.9), and those for the $C^{\alpha}H$ proton and side-chain protons are obtained in D_2O (pH 7.5–7.8). Chemical shifts are relative to internal TSP. Marks A to E show J connectivities of the $C^{\alpha}H$ proton with the $C^{\beta}H$ proton, and marks A* to E* show those of the $C^{\beta}H$ proton with the $C^{\gamma}H_3$ protons of Thr or Ile. Marks F to M show J connectivities of $C^{\alpha}H$ with one of the $C^{\beta}H_2$ protons, and marks F′ to L′ show those of $C^{\alpha}H$ with the other $C^{\beta}H$ proton of AMX-type residues. These are indicated in Figure 1. Residues marked + were not determined by the sequence-specific resonance assignment method (see text).

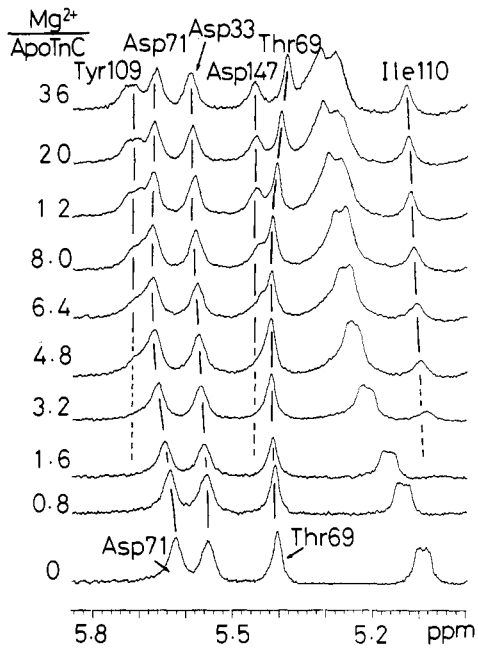

FIGURE 5: Low-field shifted $C^{\alpha}H$ proton region of ^1H NMR spectra of rabbit skeletal muscle TnC at various concentrations of Mg^{2+} added to apo-TnC. Experimental conditions are same as described in Figure 4.

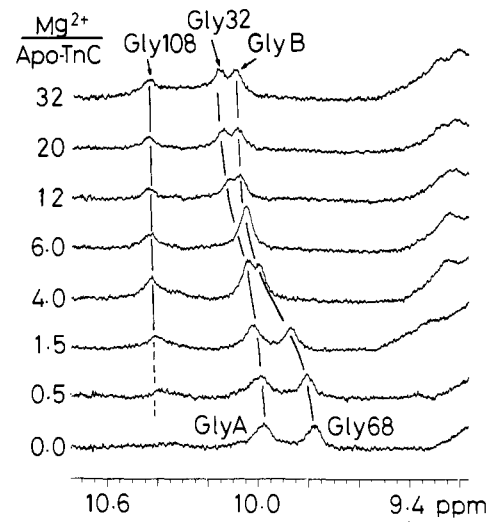

FIGURE 6: Low-field shifted amide proton region of ^1H NMR spectra of rabbit skeletal muscle TnC at various concentrations of Mg^{2+} added to apo-TnC (H_2O:D_2O = 9:1, [TnC] = 1.6 mM, [DTT] = 18 mM, [KCl] = 200 mM, 40 °C, pH 5.0–5.2, 500 MHz).

nance of δ-ring protons of Phe23 as well as Phe72 does not change appreciably.

A methyl group of Val62 of apo-TnC was already assigned in the previous work (Tsuda et al., 1988). The present work indicates that the methyl groups of Val62 and Ile34 are not affected by the addition of Mg^{2+} (data not shown). Thus, we can readily assign one of the $C^{\gamma}H_3$ protons of Val62 in the Mg^{2+}-saturated state.

Figure 5 shows a low-field region of $C^{\alpha}H$ proton resonances at various Mg^{2+} concentrations and at pH 7.5–7.8. With increasing ratio of $[Mg^{2+}]/[apo\text{-}TnC]$, $C^{\alpha}H$ resonances of Tyr109, Ile110, and Asp147 grow in intensity, and resonances of $C^{\alpha}H$ protons of Asp33, Thr69, and Asp71 shift significantly to higher or lower fields. These results are at variance with those reported by Levine et al. (1978), who reported no significant change for resonances of residues in the N-terminal domain.

Figure 6 shows an expanded view of the amide proton region of the ^1H NMR spectra in H_2O at various Mg^{2+} concentrations. The spectrum of apo-TnC is shown at the bottom and that in the Mg^{2+}-saturated state at the top. Upon the addition of Mg^{2+} up to 4.0 mol, the amide proton resonance of Gly108 appears in this region and grows in intensity. For apo-TnC, this resonance is buried in the crowded region of 8.0–8.5 ppm. A slight upfield shift of Gly108 is probably due to a pH change

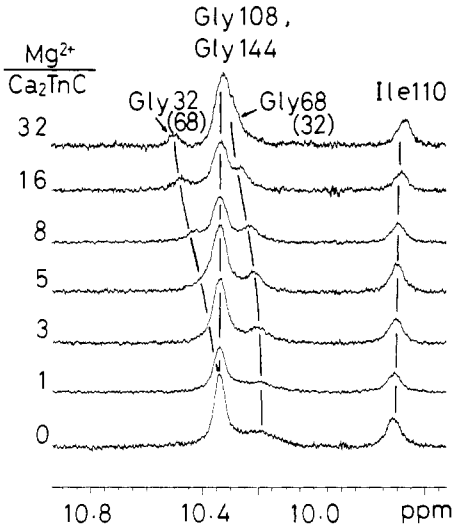

FIGURE 7: Low-field shifted amide proton region of ^1H NMR spectra of rabbit skeletal muscle TnC at various concentrations of Mg^{2+} added to Ca_2TnC (H_2O:D_2O = 9:1, [TnC] = 1.6 mM, [DTT] = 17 mM, [KCl] = 200 mM, 40 °C, pH 6.9, 500 MHz).

from 5.0 to 5.2 in the course of the titration.

As shown in Figure 6, the amide proton resonance at 9.78 ppm of Gly68 at the bottom shifts continuously to the position of GlyB at the top with increasing $[Mg^{2+}]/[$apo-TnC$]$ from 0 to 32. Thus, GlyB can be assigned to Gly68. The resonance of GlyA at the bottom shifts continuously to the position of Gly32 at the top. Thus, GlyA can be assigned to Gly32. In the previous paper, we labeled these two amide resonances m and n (Tsuda et al., 1988).

In the present work, we found that resonances of residues of not only the C domain but also the N domain are influenced by the addition of Mg^{2+} ions. These results suggest that the binding of Mg^{2+} induces conformational change in the N and C domains of TnC. The conformational change of the N domain might be induced by either (1) Mg^{2+} binding to the N domain or (2) Mg^{2+} binding to the C domain. In the following, these two possibilities are examined.

Mg^{2+} Titration of Ca_2TnC. We carried out the Mg^{2+} titration for Ca_2TnC, in which TnC binds 2 mol of Ca^{2+} to the C domain. In the course of this experiment, TnC continues to bind Ca^{2+} to the C domain, since the affinity of Ca^{2+} to the C domain is 100-fold stronger than that of Mg^{2+} (Potter & Gergely 1975; Ogawa 1985). Figure 7 shows an expanded view of the amide region of the ^1H NMR spectra at various concentrations of Mg^{2+} added to Ca_2TnC. Resonances of Gly108 and Gly144 show no change in the whole range of the titration. In addition to these Gly's, the following residues are not affected: Asp107, Tyr109, Ile110, Asp111, His125, Arg145, Ile146, Asp147, and Phe148 (data not shown here). These results indicate that two Ca^{2+} ions in the C domain are not replaced with Mg^{2+} and that no conformational change occurs in the C domain.

As shown in Figure 7, amide proton resonances of Gly32 and Gly68 shift to lower fields with increasing ratio of $[Mg^{2+}]/[Ca_2TnC]$. This behavior has a close resemblance to that observed in the Mg^{2+}-titration of apo-TnC. Similar behavior is also observed for $C^{\alpha}H$ protons of Asp33, Ser35, Thr69, and Asp71 in the N domain. These results suggest that Mg^{2+} binds to the N domain and changes the conformation of the N domain.

Mg^{2+} Titration of Ca_4TnC. We carried out the Mg^{2+}-titration experiment for TnC with 4 mol of Ca^{2+} per mol of protein, in which all four Ca^{2+}-binding sites in the N and C

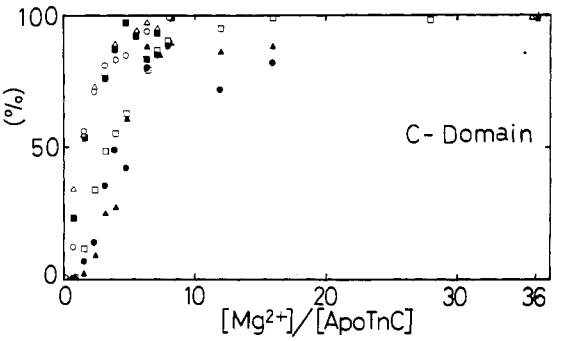

FIGURE 8: Relative change in intensity for residues of the C-terminal domain of TnC as functions of the $[Mg^{2+}]/[$apo-TnC$]$ ratio (Phe99 (■), Tyr109 (▲), His125 (○), Ile110 (□), Asp147 (●), Phe148 (△)).

domains are saturated with Ca^{2+} (Potter & Gergely, 1975). The addition of Mg^{2+} up to a total $[Mg^{2+}]/[Ca_4TnC]$ ratio of 60 does not cause any appreciable change for Phe99, Asp107, Gly108, Tyr109, His125, Gly144, and Phe148 in the C domain. These results show that Ca^{2+} ions bound to the C domain are not replaced with Mg^{2+} ions. In addition to the above-mentioned resonances, the following resonances of the N domain are not affected: (1) amide resonances of Gly32 and Gly68; (2) aromatic resonances of Tyr10, Phe23, and Phe72; and (3) methyl resonances of Ile34 and Val62. These results indicate that two Ca^{2+} ions bound to the N domain are not replaced with Mg^{2+} ions.

The fact that the addition of Mg^{2+} affects resonances of residues in the N domain of apo-TnC and Ca_2TnC but does not affect those of Ca_4TnC strongly suggests that the two N-domain Ca^{2+}-binding sites also bind Mg^{2+} ions.

Conformational Change Induced by Mg^{2+} Binding. As shown in Figure 4, PheC and Phe148 in the Mg^{2+}-bound state appear at higher fields probably due to ring current. NOE cross-peaks are also observed between ring proton resonances of these residues. These observations closely resemble those for Phe99 and Phe148 of Ca_4TnC, which also show ring current shift and NOE cross-peaks (Tsuda et al., 1988). Taking into account such similarity between Mg^{2+}- and Ca^{2+}-bound TnC's, PheC is presumably assignable to Phe99. There exists a cluster of hydrophobic residues including Phe99 and Phe148 in the C domain of Mg^{2+}-bound TnC. In the N domain the equivalent residues are Phe23 and Phe72.

The following residues can be used for probing the conformational change of the C domain induced by Mg^{2+} binding: Phe99, Asp107, Gly108, Tyr109, Ile110, Asp111, His125, Gly144, Arg145, Ile146, Asp147, and Phe148. These are located in the Ca^{2+}-binding sites and/or hydrophobic region of the C domain (Kretsinger, 1980). These results indicate that the conformation of the Mg^{2+} (Ca^{2+})-binding sites as well as the hydrophobic region changes by Mg^{2+} binding.

For residues in the N-domain of TnC, the Mg^{2+}-induced spectral change is observed for the following residues locating in the Mg^{2+} (Ca^{2+})-binding sites: Gly32, Asp33, Gly68, Thr69, and Asp71. However, no appreciable change is observed for the following residues locating in the hydrophobic region: Phe23, Ile34, Val162, and Phe72. These results suggest that the binding of Mg^{2+} changes the conformation of the Mg^{2+}(Ca^{2+})-binding sites of the N domain but does not change the conformation of the hydrophobic region of the N domain. This is in contrast to the behavior of the C domain; the corresponding hydrophobic region as well as Ca^{2+}-binding sites of the C domain changes the conformation.

Figure 8 shows the relative change in intensity normalized by the total difference as a function of the $[Mg^{2+}]/[$apo-TnC$]$

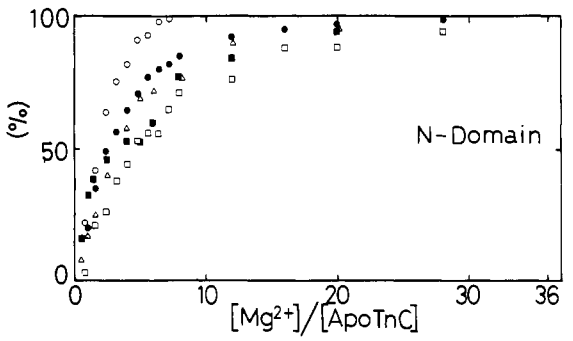

FIGURE 9: Relative changes in the chemical shift for residues of the N-terminal domain of TnC as functions of the $[Mg^{2+}]/[apo\text{-}TnC]$ ratio (Gly32 (■), Asp33 (□), Asp71 (○), Gly68 (△), Thr69 (●)).

ratio for residues in the C domain. Figure 9 shows a similar diagram for residues in the N domain, in which the relative change in chemical shift normalized by the total difference is plotted as a function of the $[Mg^{2+}]/[apo\text{-}TnC]$ ratio. From these figures, Mg^{2+}-binding constants are estimated to be on the order of 10^2–10^5 M^{-1} for both Ca^{2+}-binding sites of the N and C domains. The reported binding constants of Mg^{2+} are 10^3 M^{-1} for the C domain and 520 M^{-1} for the N domain (Ogawa, 1985).

The results obtained here indicate that the conformational exchange between Mg^{2+} free and bound states of the C domain is slower than that of the N domain. The rate of conformational exchange of the C domain is estimated to be 20–30 s^{-1} from the chemical shift difference between apo and Mg^{2+}-bound forms of C2 ring proton of His125 (the C domain). This is relatively faster than a reported value of 10 s^{-1} (Johnson et al., 1979; Drakenberg et al., 1987). A value greater than 1000 s^{-1} is obtained for the conformational exchange of the N domain by using the $C^{\alpha}H$ proton of Asp33 as a probe. These slow and fast exchange behaviors of Mg^{2+} binding have close resemblance to those of Ca^{2+} binding to apo-TnC (Tsuda et al., 1988).

It should be noted that the spectrum of apo-TnC observed in the present work is not similar to that reported by Drakenberg et al. (1987) but is similar to the spectrum that was synthesized by them from spectra of two tryptic fragments, $TR_1C(9\text{–}84)$ and $TR_2C(89\text{–}159)$. Furthermore, the slow exchange behavior observed in this work for residues in the C domain is at variance with the results observed by Drakenberg et al., who reported that both fast and slow exchange processes occur for residues of the C domain. The reason for this discrepancy is presumably the dimerization of TnC used in their work.

The reason for the wide dispersion of the data shown in Figures 8 and 9 is not clear at present.

Antiparallel β-Sheet Structure in TnC. The existence of the antiparallel β-sheet structure in Ca_2TnC was demonstrated by the recent X-ray crystal structure determination of turkey skeletal muscle TnC (Herzberg & James, 1988). The previous ^1H NMR study (Tsuda et al., 1988) revealed that the β-sheet structure exists in the N domain of apo-TnC, while in the C domain the β-sheet structure is loosely formed or destroyed. Drabikowski et al. (1985) reported the existence of the β-sheet structure in the C-terminal-half fragment in the Mg^{2+}-bound state.

Some spectral characteristics for the β-sheet structure have been proposed: (1) the low-field shift of the amide proton due to a hydrogen bond (Perkins & Wüthrich, 1979; Wagner et al., 1983); (2) the low-field shift of $C^{\alpha}H$ proton resonances (Dalgarno et al., 1983a,b; Szilágyi & Jardetzky, 1989); and (3) the existence of NOE between two proximal $C^{\alpha}H$ protons

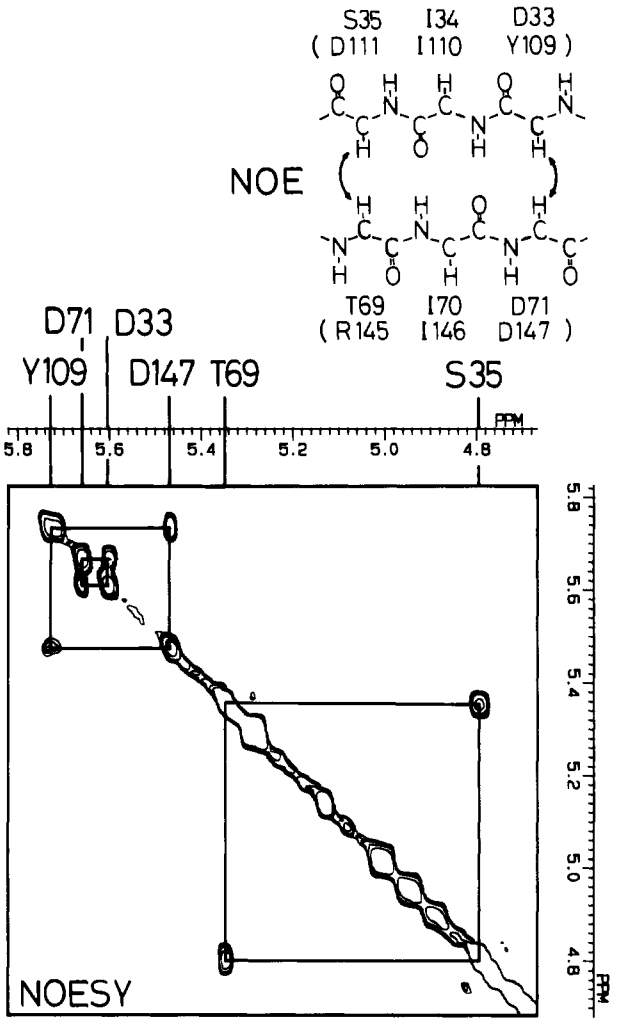

FIGURE 10: Low-field shifted $C^{\alpha}H$ proton region of the pure-phase NOESY spectrum of Mg^{2+}-bound TnC. The mixing time is 100 ms. Resonance positions of $C^{\alpha}H$ protons are indicated at the upper part of the NOESY spectrum. A schematic diagram of the β-sheet structure in the N domain is illustrated at the top.

(Pardi et al., 1983; Englander & Wand, 1987). In the present work, we examined these characteristics for Mg^{2+}-bound TnC.

As shown in Figure 2 and Table I, amide protons of Ile110 and Ile146 of Mg^{2+}-bound TnC resonate (9.24 and 9.34 ppm, respectively) at lower fields than the reported position of a "random-coil" conformation (8.2 ppm; Bundi & Wüthrich, 1979). This fact suggests that amides of Ile110 and Ile146 form hydrogen bonds. Figure 10 shows an low-field-shifted $C^{\alpha}H$-resonance region of the pure-phase NOESY spectrum of Mg^{2+}-bound TnC. $C^{\alpha}H$ proton resonances of Tyr109 and Asp147 appear at lower fields, indicating the formation of the β-sheet structure. Interresidue NOE cross-peaks are observed between $C^{\alpha}H$ protons of Tyr109 and Asp147, indicating the spatial proximity of these protons. The above results suggest that in the C domain of Mg^{2+}-bound TnC the antiparallel β-sheet structure is formed between two Ca^{2+}–Mg^{2+}-binding sites constituted by Tyr109-Ile110-Asp111 and Arg145-Ile146-Asp147. In the N domain the equivalent residues are Asp33-Ile34-Ser35 and Thr69-Ile70-Asp71, respectively.

For the N domain of Mg^{2+}-bound TnC, the following information is obtained: (1) the amide proton resonances of Ile34 and Ile70 appear at lower fields (Figure 1 and Table I); (2) the $C^{\alpha}H$ protons of Asp33, Ser35, Thr69, and Asp71 resonate at lower fields (Figures 2 and 10 and Table I); and (3) NOE's are observed between $C^{\alpha}H$ protons of Asp33 and Asp71 and between those of Ser35 and Thr69 (Figure 10).

These results suggest that Asp33-Ile34-Ser35 constitutes a β-sheet structure antiparallel to the strand of Thr69-Ile70-Asp71. The schematic diagram of this structure is depicted in the upper part of Figure 10.

Hydrogen Bonding. Amide protons of Gly32 and Gly68 of apo-TnC resonate at lower fields than the random-coil position (Bundi & Wüthrich, 1979), suggesting that these amide protons form hydrogen bonds. This is in agreement with the X-ray crystallographic results by Herzberg & James (1988). They showed that amides of Gly35 and Gly71 of turkey skeletal muscle TnC (corresponding to Gly32 and Gly68 of rabbit skeletal muscle TnC) are hydrogen bonded. For Mg^{2+}-bound TnC, we also observed the similar low-field shifts of Gly32 and Gly68. These observations may indicate that the amide protons of Gly32 and Gly68 form the hydrogen bond in Mg^{2+}-bound TnC as well.

The formation of hydrogen bonds is expected for Gly108 and Gly144 in the C domain, since these residues are equivalent to Gly32 and Gly68 in the N domain, respectively. For Ca^{2+}-bound TnC the amides of Gly108 and Gly144 have been reported to form hydrogen bonds (Tsuda et al., 1988). The amide proton resonance of Gly108 of Mg^{2+}-bound TnC appears at the lowest position (10.48 ppm) of all amide proton resonances, indicating the formation of a hydrogen bond. On the other hand, the amide of Gly144 does not show such a low-field shift (9.18 ppm). These results suggest that the amide proton of Gly144 does not form a hydrogen bond or does so weakly. In the case of apo-calmodulin (CaM), a highly homologous protein to TnC, the amide proton of Gly98 forms a hydrogen bond but that of Gly134 does not. These two Gly's of CaM correspond to Gly108 and Gly144 of TnC, respectively. The conformation of Mg^{2+}-bound TnC is similar to that of apo-CaM at this point.

Conclusions obtained in the present work are summarized as follows: (1) Two Ca^{2+}-binding sites of the N domain bind Mg^{2+} ions. These sites are not specific to Ca^{2+} only. (2) Binding of Mg^{2+} induces a conformational change in the hydrophobic region of the C domain, but does not induce a change in the hydrophobic region of the N domain. (3) The antiparallel β-sheet structure is formed in both the N and C domains of Mg^{2+}-bound TnC.

Acknowledgments

The authors thank Professor F. Morita of Hokkaido University for helping with the sample preparation. We are grateful to Dr. K. Takegoshi for taking NOESY spectra with an SR-1331 water-suppression pulse sequence.

Supplementary Material Available

Four figures with captions of 2QF-COSY, NOESY, and HOHAHA spectra of Mg^{2+}-bound TnC (6 pages). Ordering information is given on any current masthead page.

Registry No. Mg, 7439-95-4.

References

Andersson, T., Drakenberg, T., Forsén, S., & Thulin, E. (1981) *FEBS Lett. 125*, 39.

Babu, Y. S., Bugg, C. E., & Cook, W. J. (1987) in *Calcium-Binding Proteins in Health & Disease*, pp 305, Academic Press, New York.

Bax, A., & Davis, D. D. (1985) *J. Magn. Reson. 65*, 355.

Bax, A., Freeman, R., & Frenkiel, T. A. (1981) *J. Am. Chem. Soc. 103*, 2104.

Billeter, M., Brawn, W., & Wüthrich, K. (1982) *J. Mol. Biol. 155*, 321.

Bundi, A. & Wüthrich, K. (1979) *Biopolymers 18*, 285.

Collins, J. H., Potter, J. D., Horn, M. J., Wilshire, G., & Jackman, N. (1975) *J. Biol. Chem. 252*, 6356.

Dalgarno, D. C., Levine, B. A., Williams, R. J. P., Fullmer, C. S., & Wasserman, R. H. (1983a) *Eur. J. Biochem. 137*, 523.

Dalgarno, D. C., Levine, B. A., & Williams, R. J. P. (1983b) *Biosci. Rep. 3*, 443.

Drabikowski, W., Dalgarno, D. C., Levine, B. A., Gergely, J., Grabarek, Z., & Leavis, P. C. (1985) *J. Biochem. 151*, 17.

Drakenberg, T., Forsén, S., Thulin, E., & Vogel, H. J. (1987) *J. Biol. Chem. 262*, 672.

Englander, S. W. & Wand, A. J. (1987) *Biochemistry 26*, 5958.

Grabarek, Z., Leavis, P. C., & Gergely, J. (1986) *J. Biol. Chem. 261*, 608.

Herzberg, O., & James, M. N. G. (1988) *J. Mol. Biol. 203*, 761.

Ikura, M., Minowa, O., & Hikichi, K. (1985) *Biochemistry 24*, 4264.

Johnson, J. D., Charlton, S. C., & Potter, J. D. (1979) *J. Biol. Chem. 254*, 3497.

Klevit, R. E. (1985) *J. Magn. Reson. 62*, 551.

Kohama, K. (1980) *J. Biochem. (Tokyo) 88*, 591.

Kretsinger, R. H. (1980) *CRC Crit. Rev. Biochem. 8*, 119.

Levine, B. A., Thorton, J. M., Fernandes, R., Kerry, C. M., & Mercola, D. (1978) *Biochim. Biophys. Acta 535*, 11.

Mehlkopf, A. F., Korbee, D., Tiggelman, T. A., & Freeman, R. (1984) *J. Magn. Reson. 58*, 315.

Müller, N., Ernst, R. R., & Wüthrich, K. (1986) *J. Am. Chem. Soc. 108*, 6482.

Ogawa, Y. (1985) *J. Biochem. (Tokyo) 97*, 1011.

Pardi, A., Wagner, G., & Wüthrich, K. (1983) *Eur. J. Biochem. 137*, 445.

Perkins, S. J., & Wüthrich, K. (1979) *Biochim. Biophys. Acta 576*, 409.

Potter, J. D. & Gergely, J. (1975) *J. Biol. Chem. 250*, 4628.

Ribeiro, A., Parello, J., & Jardetzky, O. (1984) *Prog. Biophys. Mol. Biol. 43*, 95.

Szilágyi, L. & Jardetzky, O. (1989) *J. Magn. Reson. 83*, 441.

Szynkiewicz, J., Stepkowski, D., Brzeska, H., & Drakenberg, W. (1984) *FEBS Lett. 181*, 281.

Takegoshi, K., Tsuda, S., & Hikichi, K. (1989) *J. Magn. Reson. 85*, 198.

Tsuda, S., Hasegawa, Y., Yoshida, M., Yagi, K., & Hikichi, K. (1988) *Biochemistry 27*, 4120.

Vogel, H. J., Drakenberg, T., & Forsén, S. (1983) *NMR of NEWLY ACCESSIBLE NUCLEI 1*, 157.

Wagner, G., Pardi, A., & Wüthrich, K. (1983) *J. Am. Chem. Soc. 105*, 5948.

Wüthrich, K. (1976) in *NMR IN BIOLOGICAL RESEARCH: PEPTIDES AND PROTEINS.*

Wüthrich, K. (1983) *Biopolymers 22*, 131.

Wüthrich, K., Wider, G., Wagner, G., & Braun, W. (1982) *J. Mol. Biol. 155*, 311.

Wüthrich, K., Billeter, M., & Brawn, W. (1984) *J. Mol. Biol. 180*, 715.

Zuiderweg, E. R. P., Hallenga, K., & Olejniczak, E. T. (1986) *J. Magn. Reson. 70*, 336.